SUPPLEMENTARY APPENDIX

This appendix has been provided by the authors to give readers additional information about their work.

TABLE OF CONTENTS

LIST OF INVESTIGATORS

Clinical Trial Site: The Ohio State University Wexner Medical Center 410 W. Tenth Ave, Columbus OH 43210

Clinical Laboratory Facility: OSUCCC Pelotonia Institute for Immuno-Oncology, 460 W. 12th Ave Room 580 Biomedical Research Tower, Columbus OH 43210

Clinical Investigators: Carlos Diego Malvestutto, M.D. M.P.H; Zeinab El Boghdadly, M.D.; Mohammad Mahdee Sobhanie, M.D.; Jose Bazan, D.O.; Mark Lustberg, M.D. Ph.D.; Susan Koletar, M.D.; Zihai Li, M.D. Ph.D.; Kelsi Reynolds; Karthik Chakravathy

Complete list of contributors (alphabetical): Carter Allen[1,3,4], Jose Bazan[2], Chelsea Bolyard[3], Zeinab El Boghdadly[2], Donna Bucci[3], Karthik B. Chakravarthy[3,11], Yuzhou Chang[1,3,4], Dongjun Chung[3,4], Martin Devenport[13], John P. Evans[12], Manuja Gunasena[8,9], Aastha Khatiwada[5], Susan Koletar[2], Amrendra Kumar[6,10], Anqi Li[1,3,11], Zihai Li[2,3], Shan-Lu Liu[12], Yang Liu[13], Namal P. M. Liyanage[8,9], Mark Lustberg[2], Anjun Ma[4], Qin Ma[4], Carlos D. Malvestutto[2], Kelsi Reynolds[3], Brian P. Riesenberg[3], Mohammad Mahdee Sobhanie[2], No-Joon Song[3], Zequn Sun[5], Maria Velegraki[3], Anna E. Vilgelm[3,6,10], Kevin P. Weller[3], Menglin Xu[2], Mohamed Yusuf[6], Cong Zeng[12], Pan Zheng[13].

Affiliations:

[1]The Ohio State University, Columbus, OH 43210, USA

[2]Department of Internal Medicine, The Ohio State University College of Medicine, Columbus, OH

[3]The Pelotonia Institute for Immuno-Oncology, The Ohio State University Comprehensive Cancer Center, Columbus, OH 43210, USA

[4]Department of Biomedical Informatics, The Ohio State University College of Medicine, Columbus, OH

[5]Department of Public Health Sciences, Medical University of South Carolina, Charleston, SC

[6]The Ohio State University Comprehensive Cancer Center, Columbus, OH 43210, USA

[7]Department of Microbiology, The Ohio State University College of Arts and Sciences, Columbus, OH 43210, USA

[8]Department of Microbial Infection and Immunity, The Ohio State University College of Medicine, Columbus, OH 43210, USA

[9]Department of Veterinary Biosciences, The Ohio State University College of Veterinary Medicine, Columbus, OH 43210, USA

[10]Department of Pathology, The Ohio State University College of Medicine, Columbus, OH

[11]The Ohio State University College of Medicine, Columbus, OH 43210, USA

[12]Center for Retrovirus Research and Department of Veterinary Biosciences, The Ohio State University, Columbus, OH 43210, USA

[13]OncoC4, Rockwille, MD, USA

Author contributions are as follows (alphabetically):

Study conception and design: D Bucci, M Devenport, Z Li, SL Liu, Y Liu, C Malvestutto, NJ Song, P Zeng

Acquisition of data: D Bucci, K Chakravarthy, JP Evans, M Gunasena, A Kumar, A Li, N Liyanage, C Malvestutto, K Reynolds, BP Riesenberg, NJ Song, M Velegraki, AE Vilgelm, K Weller, M Yusuf

Analysis and interpretation of data: C Allen, Y Chang, D Chung, JP Evans, K Chakravarthy, A Khatiwada, A Kumar, A Li, Z Li, SL Liu, N Liyanage, A Ma, Q Ma, BP Riesenberg, NJ Song, Z Sun, M Velegraki, AE Vilgelm, K Weller, M Xu, C Zeng

Drafting of manuscript: C Allen, C Bolyard, K Chakravarthy, D Chung, A Kumar, Z Li, SL Liu, N Liyanage, Q Ma, C Malvestutto, BP Riesenberg, NJ Song, AE Vilgelm, K Weller

Critical revision: C Allen, C Bolyard, D Chung, Z Li, SL Liu, BP Riesenberg, NJ Song

Other: Z Li, overall supervision of study activities; AE Vilgelm, acquisition of funding and supervision of cytokine studies; M Devenport, Y Liu, P Zheng for clinical study.

SUPPLEMENTARY METHODS

PATIENTS AND TRIAL PROCEDURE. This study included samples from patients enrolled in NCT04317040 at The Ohio State University Wexner Medical Center. Patients eligible for this trial were hospitalized with COVID-19, requiring supplemental oxygen but not mechanical ventilation, and had a prior positive SARS-CoV-2 PCR test. Enrolled patients were randomized in a double-blinded fashion by the hospital pharmacist to receive either a single dose of CD24Fc antibody (480mg IV infusion) or placebo control (IV saline). Peripheral blood samples were collected from patients prior to drug infusion (D1), and at subsequent time points 1, 3, 7, 14, and 28 days after drug infusion (D2, D4, D8, D15, and D29). Patients were monitored until D29, after which they completed the study endpoint. Pertinent patient clinical information was abstracted from the internal electronic medical record database including demographic data, medical history, clinical laboratory findings, and treatment regimen for COVID-19 during hospital stay (**Table S1**). All enrolled patients were able to complete the study endpoint with no demises in either group. After enrollment and completion of the study period, two patients were excluded from analysis. One exclusion was due to a diagnosis of chronic lymphocytic leukemia (CLL) which confounded the subsequent immunological analyses. Another exclusion occurred with a patient who received an infusion but was discharged before any post-infusion peripheral blood sample could be collected; hence no comparative analysis could be made using this patient. Written or witnessed oral informed consent was obtained for each patient. This trial and protocol were approved by Western Institutional Review Board. The study was monitored continuously by a clinical monitor and a medical monitor from the contract research organization (CRO) who also generated safety reports submitted to an independent Data and Safety Monitoring Board (DSMB). Data quality control checks were performed and medical monitor verified that the clinical trial was conducted and data was generated in compliance with protocol, International Conference on Harmonization Good Clinical Practice (ICH GCP) and all applicable regulatory requirements.

Patient characteristics were clinically matched between the two groups. All patients enrolled in the study received a treatment regimen for COVID-19 by hospital care teams regardless of their placebo/CD24Fc treatment status. Patients were randomized in a double-blind fashion into CD24Fc antibody treatment group (n=10) or placebo control group (n=12).

PBMC COLLECTION AND FLOW CYTOMETRY STAINING. Samples for this study were collected from patients enrolled in clinical trial NCT04317040. We analyzed samples from 22 patients hospitalized at The Ohio State University Wexner Medical Center with severe COVID-19. Peripheral blood mononuclear cells (PBMCs) were isolated per manufacturer's protocol using CPT tubes (BD Bioscience). Healthy donor (HD) PMBCs were obtained from STEMCELL Technologies™. We utilized a 36-color flow cytometry panel (**Table S2**, developed by Cytek[1]) to distinguish immune populations; we developed a 25-color panel (**Table S2**) to study activation status of $CD8^+$, $CD4^+$, and $CD56^+$ subsets. For the 25-color panel, surface markers were stained in 4°C for 1h and FOXP3/Transcription Factor Staining Buffer Set (eBioscience™) was used per manufacturers recommendation to perform intracellular staining. Cells were analyzed using the Cytek Aurora system.

CYTOKINE AND CHEMOKINE ASSAY. Plasma samples were processed using multiplexed ELISA-based platform Quantibody® Human Inflammation Array 3 (RayBiotech QAH-INF-3) in accordance with manufacturer's protocol. Slides were shipped to manufacturer site for scanning and data extraction services. Raw optical data were analyzed using manufacturer's analysis tool to construct standard curves and determine absolute cytokine concentrations. Cytokines for which standards did not yield good standard curve fit or that were undetectable were excluded (IFNγ, IL1rα, IL2, IL13, MCP-1, TNFα, TNFβ, IL-11, IL-12p70, IL-17A). Seven of these cytokines were detected using an alternative method. Specifically, cytokines IFNγ, IL1rα, IL2, IL13, MCP-1,

TNFα, and IL-12p70 were measured by Luminex analysis. For that, plasma samples were sent to EVE Technologies that performed the assay and provided cytokine concentration data.

FLOW CYTOMETRY DATA ANALYSIS. We integrated flow cytometry marker data from all samples and arcsinh scaling was applied using OMIQ (https://www.omiq.ai/). Then, we visualized cells in a reduced two-dimensional space using the UMAP algorithm implemented in the R package uwot[3]. We adopted a multivariate t-mixture model to cluster cells based on the normalized multivariate flow cytometry marker expression[4]. For each data set, we chose the optimal number of cell clusters by selecting the model with the minimum Bayesian information criterion (BIC) score[5]. Then, we annotated cell types by visually investigating heatmaps of median marker expressions across clusters and expressions of these markers on the UMAP space.

IMMUNE CELL ACTIVATION SCORE CONSTRUCTION. To measure activation, we defined a cell-level immune cell activation score for each flow cytometry data set. We selected a subset of immune cell activation markers from the panel[6,7], and ran a principal component analysis (PCA) comparing cells from HD and baseline (Day 1) COVID patients, using these activation markers as features. We used the first principal component (PC1) as an activation score to reflect the differences in immune cell activation between groups. The loadings of each pre-selected activation marker onto PC1 were used as coefficients to compute an activation score for COVID-19 patients after baseline.

CYTOKINE SCORE CONSTRUCTION. To construct the cytokine score, we implemented a weighted sum approach, motivated by the polygenic risk score calculation in the genome-wide association study (GWAS). First, we fit a generalized linear mixed model (GLMM) of each cytokine measurement (base 10 log-transformed) on treatment, time, treatment*time, age, sex, and race

as fixed-effect terms, along with subject-level random effect terms. Second, the *p*-value for evaluating the overall difference in trends between CD24Fc and placebo groups across all the time points was calculated using the Kenward-Roger method[8]. Finally, we obtained the weighted sum of cytokine measurements using the -2 log transformed *p*-value for the trend difference as weights, motivated by the Fisher's method. We validated the above approach using the PCA and autoencoder approaches[9].

NETWORK-LEVEL ANALYSIS OF CYTOKINE DATA. We first calculated Pearson correlation coefficients between cytokines (base 10 log-transformed). Then, we constructed a network, where a node represents a cytokine and an edge between two nodes was built if the corresponding absolute correlation coefficient is larger than 0.4, a cutoff that is usually considered to be moderate correlation[10]. The weight of an edge represents the corresponding correlation coefficient. A network was built via the MetScape[11] (version 3.1.3) application in Cytoscape[12] (version 3.8.0). We evaluated the network structure and the importance of each node in the network based on an eigenvector centrality (EC) score[13] using the CytoNCA[14] (version 2.1.6) application in Cytoscape (version 3.8.0). Nodes with larger EC scores can be considered of higher importance.

STATISTICAL ANALYSIS. All data were analyzed using the R statistical package. Group comparisons were evaluated using independent sample t-test or Kruskal-Wallis test for continuous variables, and Chi-squared test for categorical variables. In the longitudinal analyses, the overall differences in trends between CD24Fc and placebo groups across all the time points were evaluated using a GLMM of each measurement on treatment, time, treatment*time, age, sex, and race as fixed-effect terms, along with patient-level random intercepts. All mixed models were fit using the lme4 package[15]. The p-value for evaluating the overall difference in trends between CD24Fc and placebo groups across all the time points was calculated using the Kenward-Roger method[8]. The observed values and trend lines are centered at the baseline.

TREATMENT GROUP DETERMINATION. The treatment group (control vs. CD24Fc) was determined by the post-infusion sera to absorb anti-CD24 antibody for staining of human $CD24^+$ cells by flow cytometry. Patient group on the CD24Fc arm was further confirmed using CD24Fc ELISA (capture antibody: purified anti-human CD24, Clone ML5, BD bioscience, Cat#555426. San Jose, CA).

REFERENCES

1. Park LM, Lannigan J, Jaimes MC. OMIP-069: Forty-Color Full Spectrum Flow Cytometry Panel for Deep Immunophenotyping of Major Cell Subsets in Human Peripheral Blood. Cytometry A 2020;97:1044-51.
2. Zeng C, Evans JP, Pearson R, et al. Neutralizing antibody against SARS-CoV-2 spike in COVID-19 patients, health care workers, and convalescent plasma donors. JCI Insight 2020;5.
3. McInnes L, Healy J, Melville J. UMAP: Uniform Manifold Approximation and Projection for Dimension Reduction. arXiv preprint arXiv:180203426v3 [statML] 2020.
4. Lo K, Brinkman RR, Gottardo R. Automated gating of flow cytometry data via robust model-based clustering. Cytometry A 2008;73:321-32.
5. Schwarz G. Estimating the Dimension of a Model. The Annals of Statistics 1978;6:461-4, 4.
6. Scott AC, Dundar F, Zumbo P, et al. TOX is a critical regulator of tumour-specific T cell differentiation. Nature 2019;571:270-4.
7. Kallies A, Good-Jacobson KL. Transcription Factor T-bet Orchestrates Lineage Development and Function in the Immune System. Trends Immunol 2017;38:287-97.
8. Kenward MG, Roger JH. Small sample inference for fixed effects from restricted maximum likelihood. Biometrics 1997;53:983-97.
9. Liou C-Y, Cheng W-C, Liou J-W, Liou D-R. Autoencoder for words. Neurocomputing 2014;139:84-96.
10. Schober P, Boer C, Schwarte LA. Correlation Coefficients: Appropriate Use and Interpretation. Anesth Analg 2018;126:1763-8.
11. Gao J, Tarcea VG, Karnovsky A, et al. Metscape: a Cytoscape plug-in for visualizing and interpreting metabolomic data in the context of human metabolic networks. Bioinformatics 2010;26:971-3.
12. Shannon P, Markiel A, Ozier O, et al. Cytoscape: a software environment for integrated models of biomolecular interaction networks. Genome Res 2003;13:2498-504.
13. Valente TW, Coronges K, Lakon C, Costenbader E. How Correlated Are Network Centrality Measures? Connect (Tor) 2008;28:16-26.
14. Tang Y, Li M, Wang J, Pan Y, Wu FX. CytoNCA: a cytoscape plugin for centrality analysis and evaluation of protein interaction networks. Biosystems 2015;127:67-72.
15. Bates D, Mächler M, Bolker B, Walker S. arXiv preprint. arXiv:14065823. 2014.
16. Lucas C, Wong P, Klein J, et al. Longitudinal analyses reveal immunological misfiring in severe COVID-19. Nature 2020;584:463-9.

SUPPLEMENTARY FIGURES

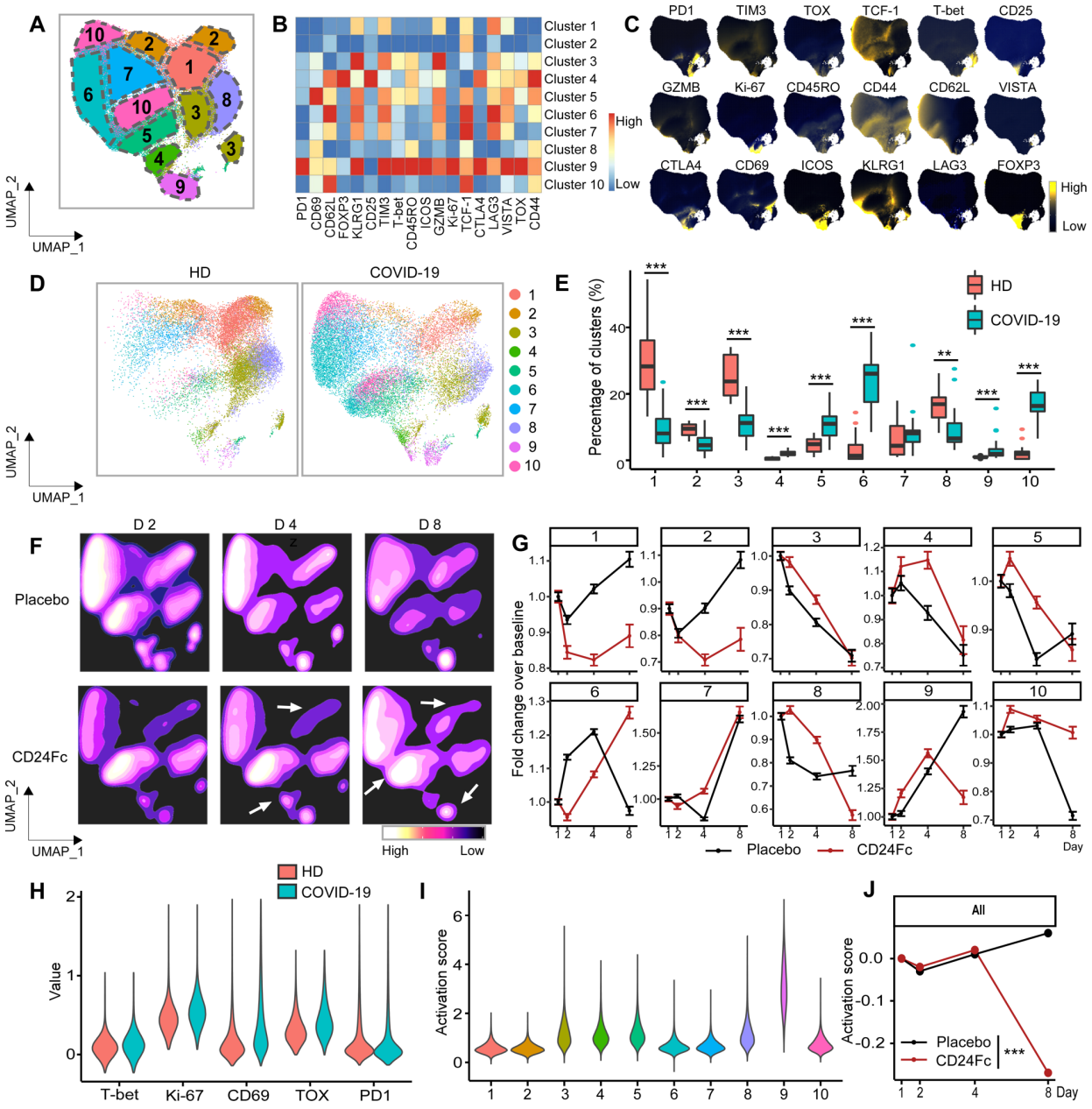

Figure S1. Subcluster analysis of peripheral blood CD4⁺ T cells in COVID-19 patients: activation following SARS-CoV2 infection is dampened by CD24Fc treatment.

We clustered 1,203,034 CD4⁺ cells from HD (n=17) and COVID-19 (n=22) patients using an unbiased multivariate *t*-mixture model, which identified 10 CD4⁺ sub-clusters that reflect statistically distinct cell activation states. We visualized the relative similarity of each cell and cell cluster on the two-dimensional UMAP space with a 10% downsampling (**Panel A**). Using median

expression of flow cytometry markers, we generated a cluster-by-marker heatmap to characterize the subsets (**Panel B**) and visualized individual marker expression patterns on the UMAP space (**Panel C**). To understand the effect of SARS-CoV2 infection on cell population dynamics, we compared UMAP dot plots (**Panel D**) and cluster frequencies (**Panel E**) of HD vs. baseline COVID-19 patient samples (cluster 1, $p<0.001$; cluster 2, $p<0.001$; cluster 3, $p<0.001$; cluster 4, $p<0.001$; cluster 5, $p<0.001$; cluster 6, $p<0.001$; cluster 8, $p=0.002$; cluster 9, $p<0.001$; cluster 10, $p<0.001$). We visualized samples from COVID-19 patients D2, 4, and 8 after CD24Fc vs. placebo treatment using contour plots to represent the density of cells throughout regions of the UMAP space (**Panel F**). We describe cluster population dynamics as fold change over baseline in each treatment group (**Panel G**; sample distribution described in **Fig 1F** legend). To better characterize the activation status of CD4 T cells, we linearly transformed a subset of markers (T-bet, Ki-67, CD69, TOX, PD1) to create a univariate cell-level activation score (**Panel H**), where highly activated cell clusters (such as cluster 9) had highest activation scores (**Panel I**). We then fit a GLMM to our longitudinal cell-level activation scores to assess the effect of CD24Fc treatment on activation scores over time (**Panel J**; $p<0.001$). The p-value for evaluating the overall difference in trends between CD24Fc and placebo groups across all time points was calculated using the Kenward-Roger method. Using this model, we found that CD24Fc-treated samples had significantly lower $CD4^+$ cell activation levels relative to placebo. **, $p<0.01$; ***, $p<0.001$.

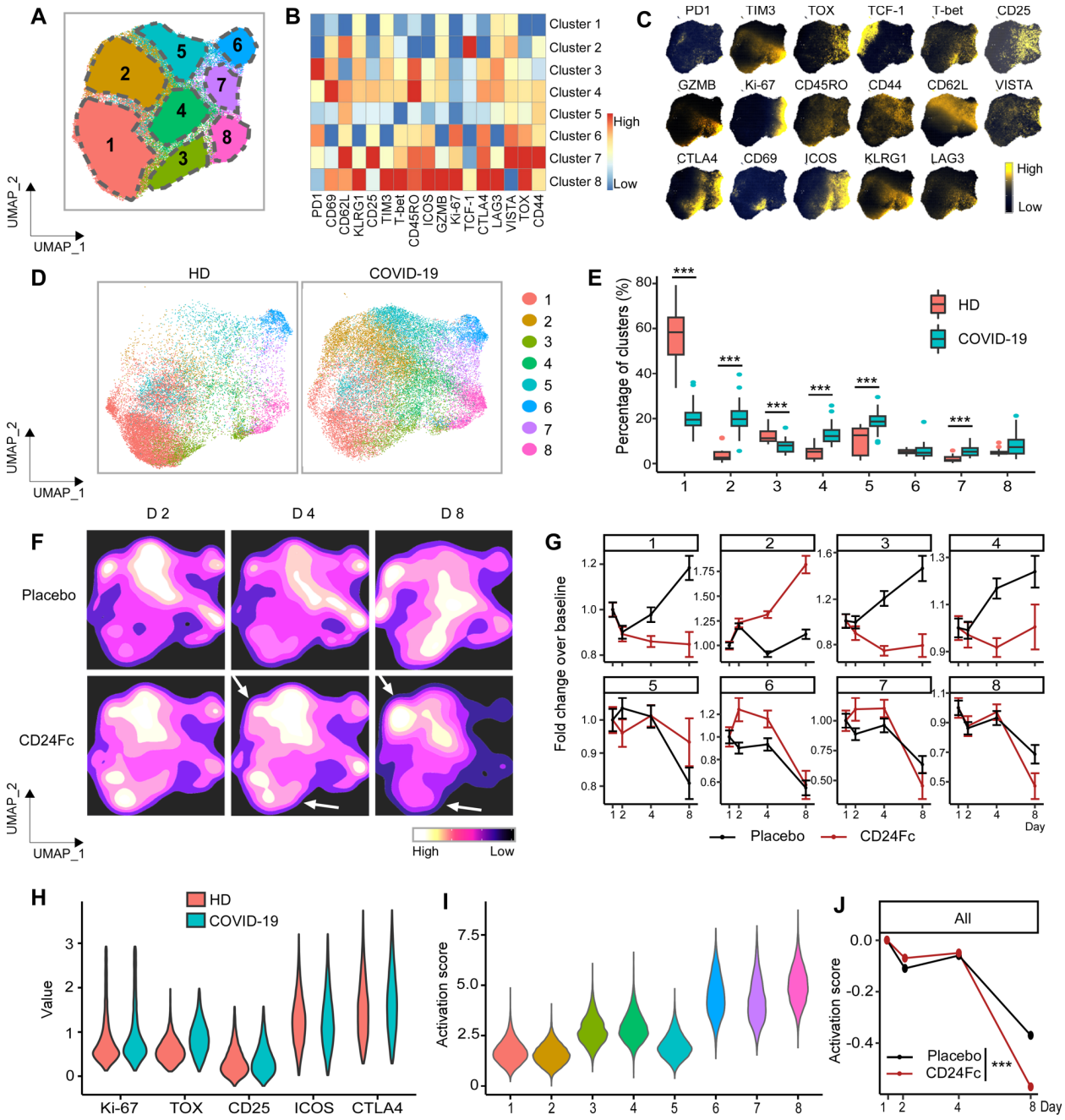

Fig S2. Subcluster analysis of peripheral blood FOXP3⁺ Treg cells in COVID-19 patients: activation following SARS-CoV2 infection is dampened by CD24Fc treatment.

We clustered 98,525 FOXP3+ Treg cells from HD (n=17) and COVID-19 (n=22) patients using an unbiased multivariate *t*-mixture model, which identified 8 FOXP3⁺ Treg sub-clusters that reflect statistically distinct cell activation states. We visualized the relative similarity of each cell and cell cluster on the two-dimensional UMAP space with a 10% downsampling (**Panel A**). Using median

expression of flow cytometry markers, we generated a cluster-by-marker heatmap to characterize the subsets (**Panel B**) and visualized individual marker expression patterns on the UMAP space (**Panel C**). To understand the effect of SARS-CoV2 infection on cell population dynamics, we compared UMAP cluster frequencies of HD vs. baseline COVID-19 patient samples (**Panels D** and **E**). We visualized samples from COVID-19 patients D2, 4, and 8 after CD24Fc vs. placebo treatment using contour plots to represent the density of cells throughout regions of the UMAP space (**Panel F**). We describe cluster population dynamics as fold change over baseline in each treatment group (**Panel G**; sample distribution described in **Fig 1F** legend). To better characterize the activation status of Treg cells, we linearly transformed a subset of markers (Ki-67, TOX, CD25, ICOS, CTLA4) to create a univariate cell-level activation score (**Panel H**), where highly activated cell clusters (such as clusters 6, 7 and 8) had highest activation scores (**Panel I**). We then fit a GLMM to our longitudinal cell-level activation scores to assess the effect of CD24Fc treatment on activation scores over time (**Panel J**). The p-value for evaluating the overall difference in trends between CD24Fc and placebo groups across all time points was calculated using the Kenward-Roger method. Using this model, we found that CD24Fc-treated samples had significantly lower Treg cell activation levels relative to placebo.

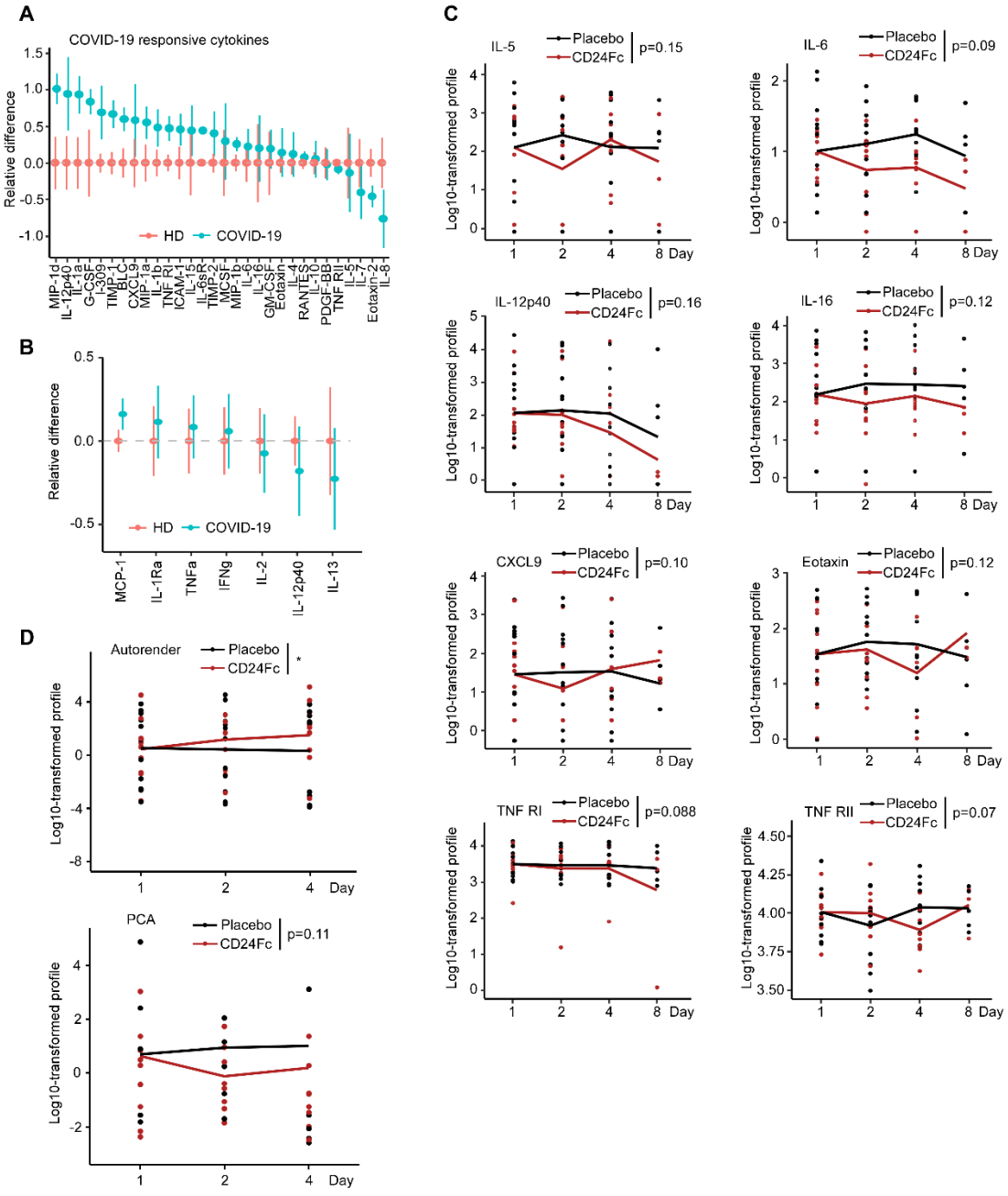

Figure S3. CD24Fc treatment downregulates systemic cytokines response in patients with COVID-19. We studied plasma cytokine and chemokine levels in HD and COVID-19 patients. Cytokine/chemokine measurements were log-transformed, and relative differences in cytokines in COVID-19 (n=22) compared to HD (n=25) samples were depicted (**Panel A**). Independent sample t-test was used to evaluate equality of average cytokine/chemokine levels. A number of

other markers displayed trends towards decline in CD24Fc cohort compare to placebo, although these changes were not statistically significant (**Panel B**). Log-10 transformed cytokine measurement (dots) and GLMM predicted fixed effects trends (lines) of IL-5, IL-6, IL-12p40, IL-16, CXCL9, Eotaxin, TNF R1 and TNF RII plasma concentrations in CD24Fc (red) and placebo (black) groups are displayed. The observed values and trend lines are centered at D1 mean. Longitudinal analysis of cytokine score was confirmed using both Autoencoder and PCA approaches (**Panel C**). We applied PCA and autoencoder on the base 10 log-transformed, centered and scaled cytokine data, and investigated the first two principal components (PCs) from the PCA and the three latent components from the autoencoder as cytokine scores. The autoencoder analysis was implemented using the Keras package. Specifically, we set one hidden layer for encoder and decoder, respectively, and three-dimensional embedding as latent layer output. All parameters were trained based on a 3-fold cross-validation. Due to missing data on D8, only D1, D2, and D4 data were used for the cytokine score calculation. For **Panels B** and **C**, the overall differences in trends between CD24Fc and placebo groups across all the time points were evaluated using a GLMM of each measurement. The p-value for evaluating the overall difference in trends between CD24Fc and placebo groups across all the time points was calculated using the Kenward-Roger method.

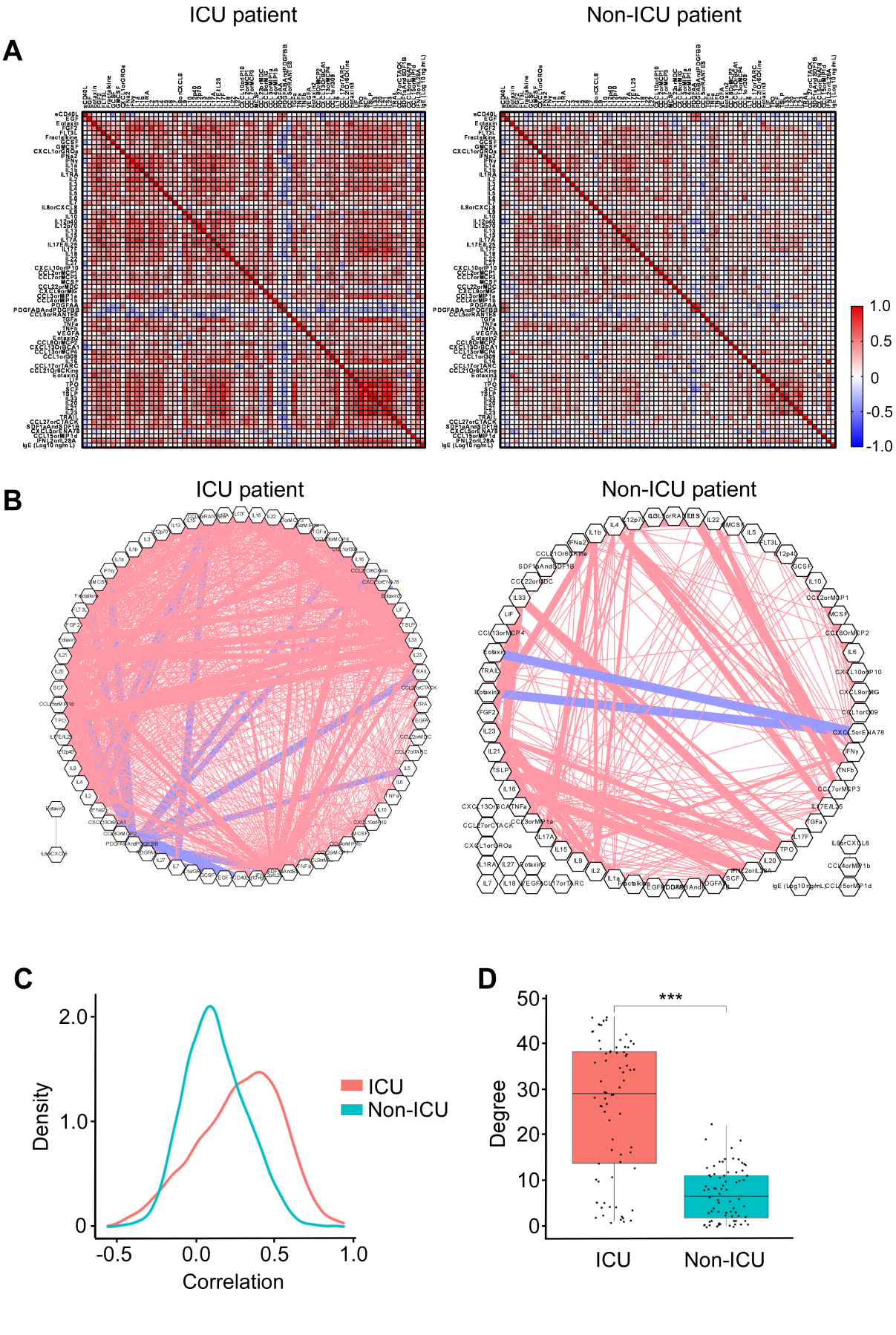
A
ICU patient
Non-ICU patient
1.0
0.5
0
-0.5
-1.0
B
ICU patient
Non-ICU patient
C
Density
2.0
1.0
0
-0.5
0.0
0.5
1.0
Correlation
ICU
Non-ICU
D
Degree
50
40
30
20
10
0
***
ICU
Non-ICU

Figure S4. Patients with severe COVID-19 that require an ICU treatment display increased correlation and connectivity of the systemic cytokine network. We analyzed correlation (A) and connectivity (B) between circulating cytokines and chemokines in COVID-19 patients that either required (ICU patients), or did not require an ICU treatment (non-ICU patients). Cytokine measurements were obtained from previously published dataset [16]. Analysis was performed as described in Fig. 4.A density plot constructed based on connectivity between plasma cytokines is shown in panel C. Panel D shows an association between the severity of COVID-19 infection and the degree of the connectivity between plasma cytokines with severe UCU cases displaying higher degree of connectivity. The p-value was calculated using Wilcoxon Rank Sum test.

SUPPLEMENTARY TABLES

Table S1. Patient Characteristics.

CHARACTERISTIC **a) Demographics**	OVERALL (N=22)	PLACEBO (N=12)	CD24Fc (N=10)	P-value
BMI - median (IQR)	31.65 (28.18-38.83)	31.65 (29.41-39.52)	32.2 (28.1-37.88)	0.644
Age, yr - median (IQR)	57 (50.25-74.75)	60.5 (53.5-75)	55 (49.5-62)	0.62
<65 yr - no. (%)	15 (68.2)	7 (58.3)	8 (80.0)	
≥65 yr - no. (%)	7 (31.8)	5 (41.7)	2 (20.0)	
Sex - no. (%)				0.903
Female	8 (36.4)	5 (41.7)	3 (30.0)	
Male	14 (63.6)	7 (58.3)	7 (70.0)	
Race - no. (%)				0.528
White	16 (72.7)	9 (75.0)	7 (70.0)	
Black/AA	5 (22.7)	2 (16.7)	3 (30.0)	
Not Specified	1 (4.5)	1 (8.3)	0 (0.0)	
Ethnicity - no. (%)				0.724
Hispanic	4 (18.2)	3 (25.0)	1 (10.0)	
Non-Hispanic	18 (81.8)	9 (75.0)	9 (90.0)	
Smoking Hx - no. (%)	7 (31.8)	3 (25.0)	4 (40.0)	0.77
b) Co-existing Conditions				
Comorbidities - no. (%)				
Obesity (BMI ≥30)	12 (54.5)	7 (58.3)	5 (50.0)	1
Hypertension	11 (50.0)	5 (41.7)	6 (60.0)	0.669
Hyperlipidemia	8 (36.4)	5 (41.7)	3 (30.0)	0.903
Heart Disease	7 (31.8)	2 (16.7)	5 (50.0)	0.226
Diabetes	7 (31.8)	3 (25.0)	4 (40.0)	0.77
Autoimmune Condition	3 (13.6)	3 (25.0)	0 (0.0)	0.281
Cancer	2 (9.1)	1 (8.3)	1 (10.0)	1
HIV	1 (4.5)	0 (0.0)	1 (10.0)	0.926
COPD/Asthma	2 (9.1)	1 (8.3)	1 (10.0)	1
c) Clinical Information				
Baseline diastolic blood pressure, mm Hg - median (IQR)	65.5 (61.5-74)	67.5 (62.5-72)	65.5 (61.75-73.25)	0.766
Baseline systolic blood pressure, mm Hg - median (IQR)	127 (121-139.75)	138.5 (117.5-144)	124 (121.75-129)	0.137
Normotensive (<130) - no. (%)	12 (54.5)	5 (41.7)	7 (70.0)	0.369
Hypertensive (≥130) - no. (%)	10 (45.5)	7 (58.3)	3 (30.0)	
Baseline O_2 saturation on room air, % - median (IQR)	0.88 (0.84-0.9)	0.86 (0.8-0.88)	0.88 (0.85-0.9)	0.185
Hypoxic (<90) - no. (%)	16 (72.7)	10 (83.3)	6 (60.0)	0.458
Non-hypoxic (≥90) - no. (%)	6 (27.3)	2 (16.7)	4 (40.0)	

Baseline respiratory rate, respirations/min - median (IQR)	20 (18-25.5)	22 (19.5-28.5)	19 (16.5-21.5)	0.053
Eupnic (≤20) - no. (%)	13 (59.1)	6 (50.0)	7 (70.0)	0.607
Tachypnic (>20) - no. (%)	9 (40.9)	6 (50.0)	3 (30.0)	
Baseline heart rate, beats/min - median (IQR)	82.5 (67-91.75)	82.5 (73-91.25)	77.5 (66.25-92.5)	0.817
Eucardic (≤100) - no. (%)	22 (100.0)	12 (100.0)	10 (100.0)	n/a
Tachycardic (>100) - no. (%)	0 (0.0)	0 (0.0)	0 (0.0)	
Baseline temperature, °C - median (IQR)	37 (36.8-37.38)	36.95 (36.77-37.12)	37.15 (36.82-37.55)	0.466
Febrile (>37.0) - no. (%)	9 (40.9)	4 (33.3)	5 (50.0)	0.722
Non-febrile (≤37.0) - no. (%)	13 (59.1)	8 (66.7)	5 (50.0)	
Baseline RBC Count, M/µL - median (IQR)	4.61 (4.36-4.94)	4.61 (4.26-4.94)	4.62 (4.44-4.94)	0.598
Low (<4.3) - no. (%)	4 (18.2)	3 (25.0)	1 (10.0)	0.541
Normal (4.3-5.5) - no. (%)	15 (68.2)	8 (66.7)	7 (70.0)	
Elevated (>5.5) - no. (%)	3 (13.6)	1 (8.3)	2 (20.0)	
Baseline WBC Count, K/µL - median (IQR)	5.75 (5.23-8.07)	6.79 (5.34-7.98)	5.62 (4.85-8.78)	0.429
Low (<4.5) - no. (%)	2 (9.1)	0 (0.0)	2 (20.0)	0.124
Normal (4.5-11.0) - no. (%)	19 (86.4)	12 (100.0)	7 (70.0)	
Elevated (>11.0) - no. (%)	1 (4.5)	0 (0.0)	1 (10.0)	
Baseline Neutrophils, K/µL - median (IQR)	4.43 (3.9-6.8)	4.93 (4.3-6.38)	4.03 (3.15-6.75)	0.323
Baseline Lymphocytes, K/µL - median (IQR)	1.04 (0.76-1.33)	1.14 (0.69-1.6)	0.92 (0.85-1.21)	0.921
Baseline Monocytes, K/µL - median (IQR)	0.36 (0.29-0.57)	0.32 (0.25-0.5)	0.38 (0.34-0.57)	0.235
Baseline Eosinophils, K/µL - median (IQR)	0.04 (0.04-0.06)	0.04 (0.04-0.04)	0.04 (0.04-0.06)	0.129
Baseline Basophils, K/µL - median (IQR)	0.04 (0.04-0.04)	0.04 (0.04-0.04)	0.04 (0.04-0.04)	0.097
Baseline Hemoglobin, g/dL - median (IQR)	13.4 (12.95-14)	13.3 (12.7-14.15)	13.45 (13.17-13.67)	0.575
Low (<13.2) - no. (%)	8 (36.4)	5 (41.7)	3 (30.0)	0.263
Normal (13.2-16.4) - no. (%)	12 (54.5)	5 (41.7)	7 (70.0)	
Elevated (>16.4) - no. (%)	2 (9.1)	2 (16.7)	0 (0.0)	
Baseline Platelet Count, K/µL - median (IQR)	224.5 (187.75-253)	224 (171.75-251)	224.5 (208.25-268.75)	0.621
Normal (150-450) - no. (%)	21 (95.5)	11 (91.7)	10 (100.0)	1
Elevated (>450) - no. (%)	1 (4.5)	1 (8.3)	0 (0.0)	
Baseline D-dimer, µg/mL - median (IQR)	0.95 (0.58-1.92)	1.12 (0.69-1.65)	0.79 (0.45-1.82)	0.276
Normal (<0.50) - no. (%)	5 (22.7)	1 (8.3)	4 (40.0)	0.21
Elevated (≥0.50) - no. (%)	17 (77.3)	11 (91.7)	6 (60.0)	
Baseline International Normalized Ratio, sec - median (IQR)	1.1 (1-1.1)	1.1 (1-1.15)	1.1 (1-1.1)	0.487

Normal (0.9-1.1) - no. (%)	17 (77.3)	9 (75.0)	8 (80.0)	1
Elevated (>1.1) - no. (%)	5 (22.7)	3 (25.0)	2 (20.0)	
Baseline ESR, mm/hr - median (IQR)	51.5 (40-71)	43 (35.75-61.5)	64.5 (43.75-71)	0.198
Baseline CRP, mg/L - median (IQR)	80.59 (68.91-142.69)	80.59 (67.83-147.37)	90.22 (72.53-132.12)	0.895
Baseline Troponin, ng/mL - median (IQR)	0.01 (0.01-0.02)	0.01 (0.01-0.01)	0.01 (0.01-0.03)	0.193
Time from symptom onset to infusion, days - median (IQR)	10.5 (8.25-12.75)	10.5 (8.75-13)	10.5 (8.25-11)	0.571
Earlier (≤10) - no. (%)	11 (50.0)	6 (50.0)	5 (50.0)	1
Later (>10) - no. (%)	11 (50.0)	6 (50.0)	5 (50.0)	
Time from infusion to discharge, days - median (IQR)	6 (4-8.75)	6 (3.75-9)	5.5 (4-7.5)	0.618
Shorter (≤7) - no. (%)	15 (68.2)	8 (66.7)	7 (70.0)	1
Longer (>7) - no. (%)	7 (31.8)	4 (33.3)	3 (30.0)	
Total hospital stay, days - median (IQR)	9 (6-11.75)	9.5 (7.5-12.25)	7 (6-10)	0.371
Shorter (≤10) - no. (%)	15 (68.2)	7 (58.3)	8 (80.0)	0.531
Longer (>10) - no. (%)	7 (31.8)	5 (41.7)	2 (20.0)	
O_2 requirement at admission, L/min - median (IQR)	2 (2-4)	2 (2-8)	2.5 (2-3.25)	0.601
None (<1) - no. (%)	5 (22.7)	3 (25.0)	2 (20.0)	0.598
Low (1-49) - no. (%)	16 (72.7)	8 (66.7)	8 (80.0)	
High (≥50) - no. (%)	1 (4.5)	1 (8.3)	0 (0.0)	
Peak O_2 requirement during hospital stay, L/min - median (IQR)	6.5 (3.25-11.25)	8.5 (4.5-26.25)	5 (3.25-6.75)	0.119
Low (1-49) - no. (%)	18 (81.8)	9 (75.0)	9 (90.0)	0.724
High (≥50) - no. (%)	4 (18.2)	3 (25.0)	1 (10.0)	
O_2 requirement at discharge, L/min - median (IQR)	3 (3-3)	3 (3-3)	3 (2-3)	0.414
None (<1) - no. (%)	17 (77.3)	10 (83.3)	7 (70.0)	0.816
Low (1-49) - no. (%)	5 (22.7)	2 (16.7)	3 (30.0)	
ICU Stay - no. (%)	5 (22.7)	4 (33.3)	1 (10.0)	0.43
d) Concomitant Medication				
Concurrent COVID-19 Treatments - no. (%)				
Convalescent Plasma	19 (86.4)	10 (83.3)	9 (90.0)	1
Remdesivir	19 (86.4)	11 (91.7)	8 (80.0)	0.865
Dexamethasone	15 (68.2)	9 (75.0)	6 (60.0)	0.77
Anti-microbials	16 (72.7)	9 (75.0)	7 (70.0)	1

Median and Inter-quartile range (IQR) was determined for all continuous variables. P-values were obtained using Kruskal Wallis test continuous variables. Chi-square test was used to obtain p-values for categorical variables.

Table S2. Immune Cell Marker Panels.

Cytek Flow Cytometry Panel	
Marker	**Description**
CD45RA	BUV395 Mouse Anti-Human CD45RA
Viability dye	LIVE/DEAD™ Fixable Blue Dead Cell Stain Kit, for UV excitation
CD16	BUV496 Mouse Anti-Human CD16
CCR5	BUV563 Mouse Anti-Human CD195 (CCR5)
CD11c	BUV661 Mouse Anti-Human CD11c
CD56	BUV737 Mouse Anti-Human CD56
CD8	BD Horizon™ BUV805 Mouse Anti-Human CD8
CCR7	Brilliant Violet 421™ anti-human CD197 (CCR7) Antibody
CD123	CD123 Monoclonal Antibody (6H6), Super Bright 436, eBioscience™
CD161	CD161 Monoclonal Antibody (HP-3G10), eFluor 450, eBioscience™
IgD	BV480 Mouse Anti-Human IgD
CD3	Brilliant Violet 510™ anti-human CD3 Antibody
CD20	CD20 Monoclonal Antibody (HI47), Pacific Orange
IgM	Brilliant Violet 570™ anti-human IgM Antibody
IgG	BD Horizon™ BV605 Mouse Anti-Human IgG
CD28	Brilliant Violet 650™ anti-human CD28 Antibody (clone CD28.2)
CCR6	Brilliant Violet 711™ anti-human CD196 (CCR6) Antibody
CXCR5	BV750 Rat Anti-Human CXCR5 (CD185)
PD-1	Brilliant Violet 785™ anti-human CD279 (PD-1) Antibody
CD141	BD Horizon™ BB515 Mouse Anti-Human CD141
CD57	FITC anti-human CD57 Antibody
CD14	Spark Blue™ 550 anti-human CD14 Antibody
CD45	CD45 Monoclonal Antibody (H130), PerCP
CD11b	PerCP/Cyanine5.5 anti-human CD11b Antibody
TCR gd	TCR gamma/delta Monoclonal Antibody (B1.1), PerCP-eFluor 710, eBioscience™
CD25	CD25 Monoclonal Antibody (BC96), PE, eBioscience™
CD4	cFluor 568 Anti-human CD4
CD24	CD24 Monoclonal Antibody (eBioSN3 (SN3 A5-2H10)), PE-eFluor 610, eBioscience™
CD95	CD95 (APO-1/Fas) Monoclonal Antibody (DX2), PE-Cyanine5, eBioscience™
CXCR3	CD183 (CXCR3) Monoclonal Antibody (CEW33D), PE-Cyanine7, eBioscience™
CD27	CD27 Monoclonal Antibody (O323), APC, eBioscience™
CD1c	Alexa Fluor® 647 anti-human CD1c Antibody
CD19	Spark NIR™ 685 anti-human CD19 Antibody
CD127	APC-R700 Mouse Anti-Human CD127
HLA-DR	HLA-DR Monoclonal Antibody (L243), APC-eFluor 780, eBioscience™
CD38	CD38 APC-Fire810
Immune Monitoring Cytometry Panel	
Marker	**Description**
Viability dye	LIVE/DEAD™ Fixable Blue Dead Cell Stain Kit, for UV excitation
CD45	CD45 Monoclonal Antibody (2D1), Super Bright 645, eBioscience™

CD3	BUV395 Mouse Anti-Human CD3 Clone SK7
CD8	CD8a Monoclonal Antibody (OKT8 (OKT-8)), Super Bright 436, eBioscience™
CD4	CD4 Monoclonal Antibody (RPA-T4), PerCP-Cyanine5.5, eBioscience™
FOXP3	FOXP3 Monoclonal Antibody (PCH101), eFluor 450, eBioscience™
CD11b	BUV661 Rat Anti-CD11b Clone M1/70
CD56	Brilliant Violet 750™ anti-human CD56 (NCAM) Antibody
CD45RO	BB515 Mouse Anti-Human CD45RO Clone UCHL1
CD25	CD25 Monoclonal Antibody (BC96), Super Bright 600, eBioscience™
PD1	BUV737 Mouse Anti-Human CD279 (PD-1) Clone EH12.1
Tim3	CD366 (TIM3) Monoclonal Antibody (F38-2E2), Super Bright 702, eBioscience™
TOX	TOX Antibody, anti-human/mouse, APC, REAfinity™
TCF1	PE anti-TCF1 (TCF7) Antibody
CD44	APC/Cyanine7 anti-mouse/human CD44 Antibody
CD62L	BV421 Mouse Anti-Human CD62L Clone DREG-56
CTLA4	PE/Dazzle™ 594 anti-human CD152 (CTLA-4) Antibody
Lag-3	CD223 (LAG-3) Monoclonal Antibody (3DS223H), PE-Cyanine5, eBioscience™
Klrg1	Brilliant Violet 510™ anti-mouse/human KLRG1 (MAFA) Antibody
T-bet	BV786 Mouse Anti-T-bet Clone O4-46
Ki-67	Ki-67 Monoclonal Antibody (SolA15), PerCP-eFluor 710, eBioscience™
GzmB	Granzyme B Monoclonal Antibody (N4TL33), Alexa Fluor 532, eBioscience™
VISTA	VISTA Monoclonal Antibody (B7H5DS8), PE-Cyanine7, eBioscience™
ICOS	Alexa Fluor® 488 anti-human/mouse/rat CD278 (ICOS) Antibody
CD69	BUV805 Mouse Anti-Human CD69 Clone FN50

Table S3. First principal component (PC1) loadings of each activation marker were used as coefficients for defining the activation score.

Marker	PC1 loading for HD & COVID D1	Average Log-Fold Change (HD vs. COVID day 1)	Wilcoxon p-value (HD vs. COVID day 1)
CD8+ T cells			
T-bet	0.71	0.52	<0.001
Ki-67	0.39	0.46	<0.001
CD69	0.28	0.39	<0.001
TOX	0.40	0.31	<0.001
GZMB	0.31	0.20	<0.001
CD4+ T cells (total)			
T-bet	0.14	0.08	<0.001
Ki67	0.69	0.38	<0.001
CD69	0.34	0.41	<0.001
TOX	0.33	0.19	<0.001
PD1	0.53	0.11	<0.001
Treg cells			
Ki-67	0.76	0.33	<0.001
TOX	0.14	0.38	<0.001
CD25	0.07	0.09	<0.001
iCOS	0.43	0.17	<0.001
CTLA4	0.47	0.30	<0.001
NK cells			
TOX	0.16	0.42	<0.001
GZMB	0.07	0.28	<0.001
KLRG1	0.08	0.06	<0.001
Ki-67	0.89	0.84	<0.001
LAG3	0.03	0.08	<0.001

Table S4. Centrality ranks of filtered and weighted correlations.

Cytokine markers	HD	D1	Placebo	CD24Fc	var	Mean
IL-5	1	1	1	9	16	3
MIP-1d	17	2	12	1	60.67	8
IL-1b	11	3	2	2	19	4.5
IL-8	2	4	8	17	44.25	7.75
G-CSF	20	5	9	4	53.67	9.5
IL-16	15	6	4	6	24.25	7.75
MIG	16	7	17	5	37.58	11.25
IL-4	10	8	6	3	8.92	6.75
MCSF	24	9	13	16	40.33	15.5
IL-12p40	14	10	5	7	15.33	9
IL-15	13	11	7	8	7.58	9.75
IL-1a	7	12	11	12	5.67	10.5
TNF RI	25	13	14	14	32.33	16.5
I-309	8	14	3	11	22	9
MIP-1a	12	15	21	13	16.25	15.25
BLC (CXCL13)	27	16	25	15	37.58	20.75
TNF RII	22	17	18	21	5.67	19.5
IL-6sR	30	18	28	22	30.33	24.5
IL-7	5	19	19	24	66.92	16.75
MIP-1b	19	20	27	30	28.67	24
IL-6	6	21	20	28	84.92	18.75
PDGF-BB	9	21	22	18	35	17.5
RANTES	18	23	23	19	6.92	20.75
GM-CSF	4	24	16	25	94.25	17.25
TIMP-1	23	25	24	20	4.67	23
IL-10	3	26	15	26	120.33	17.5
Eotaxin-2 (CCL24)	30	27	30	30	2.25	29.25
ICAM-1	30	28	26	23	8.92	26.75
Eotaxin (CCL11)	26	29	10	10	103.58	18.75
TIMP-2	21	30	29	27	16.25	26.75

HD, Healthy donor; D1, baseline COVID-19 patients; Var, variance.

Centrality scores ranked from highest (1, red) to lowest (30, blue). Variance and means calculated based on rank.